LUPINE PUBLISHERS

An archive of organic and inorganic chemical sciences

DOI: 10.32474/AOICS.2021.05.000219

ISSN: 2637-4609

Research Article

# Cooperative Effect of Cyclometalating and Ancillary Ligands to Adjust the Emission Color of Cationic Ir (III) Complexes

**Felipe Salas[1], Mireya Santander-Nelli[1], Denis Fuentealba[2], Jeronimo R. Maze[3], Iván González[4]* and Paulina Dreyse[1]***

[1]*Departamento de Química, Universidad Técnica Federico Santa María, Chile*

[2]*Facultad de Química y de Farmacia, Pontificia Universidad Católica de Chile, Chile*

[3]*Facultad de Física, Pontificia Universidad Católica de Chile, Chile*

[4]*Departamento de Química, Facultad de Ciencias Naturales, Matemática y del Medio Ambiente, Universidad Tecnológica Metropolitana, Chile*

***Corresponding author:** Paulina Dreyse, Departamento de Química, Universidad Técnica SantaMaría, Chile

Departamento de Química, Facultad de Ciencias Naturales, Matemática y del Medio Ambiente, Universidad Técnica Santa María, Chile

**Received:** September 15, 2021 **Published:** October 11, 2021

## Abstract

A series of Ir (III) complexes $[Ir(F_2ppy)_2(neo)](PF_6)$ $(C_1)$, $[Ir(F_2ppy)_2(biq)](PF_6)$ $(C_2)$, $[Ir(F_2ppy)_2(dabiq)](PF_6)$ $(C_3)$, $[Ir(bzq)_2(neo)](PF_6)$ $(C_4)$, $[Ir(bzq)_2(biq)](PF_6)$ $(C_5)$, $[Ir(bzq)_2(dabiq)](PF_6)$ $(C_6)$, have been synthesized and their photophysical properties were investigated supported by theoretical calculations to propose emitters based on single complex or host-guest blend to potential applications in LEC devices. In acetonitrile, C1 and C4 showed emissions at higher energies (490-515 nm); C2 and C3 emitted ~580 nm and C5 and C6 at low energy (~615 nm). C1 reached the higher quantum yield (43%) and lower values (3-5%) were obtained with C5 and C6. The photophysical differences are consistent with cyclometalating and ancillary ligand natures, since both are involved in the triplet emitting states. The experimental and theoretical evaluation allow us to propose C1 and C3 as promising individual blue and yellow-orange emitters, respectively, as well as single and double host-guest doped systems, with blends of (C1), (C2), (C3), (C4), (C5) and (C6), respectively, to produce white emissions.

**Keywords:** Density Functional Calculations; Iridium (III) Complexes; Light Emitting Electrochemical Cell; Luminescence; Tunable emission energies.

## Introduction

The luminescent properties of ionic Transition Metal Complexes (iTMCs) are take advantage in several energy conversion applications, among which Light Emitting Electrochemical Cells (LECs) is stand out. [1] These devices arise from the evolution of LEDs (Light Emitting Diodes) and OLEDs (Organic Light Emitting Diodes) [2], being characteristic in LECs the simplified fabrications that involve a single emissive layer of an iTMC between a metallic cathode and anode [3,4]. In addition, these devices can operate with low-bias and with air-stable cathodic materials avoiding encapsulation processes [5-7]. The working mechanism of LECs comprise hole-electron recombination processes: under the influence of an electrical field, the electrons are injected directly from the cathode into the LUMO (Lowest Unoccupied Molecular Orbital) of the iTMC and the holes are introduced from the anode into the HOMO (Highest Occupied Molecular Orbital)[4] The carriers hop toward one another and if both charges arrive in a single molecule a molecular excited state may be formed, and the recombination process takes place emitting light if the deactivation is by radiative way [8].

The cyclometalated Ir (III) complexes of the type $[Ir(C^N)_2(N^N)]^+$, (C^N: cyclometalating and N^N: ancillary ligands) stand out as iTMCs in LECs due to their attractive photophysical properties, strongly influenced by the spin-orbit coupling exerted by Ir (III) core, promoting intense emissions with excited-states of short lifetimes [9]. The emission energies are modulated by electron donor-acceptor nature of the chelating ligands since both N^N and C^N have contributions on the frontier molecular orbitals [10,11]. In general, the LUMO is mainly composed by $\pi^*$-orbitals

of N^N ligands and HOMO usually has the electronic density in the C^N ligands and Iridium center [12]. Consequently, low-energy electronic transitions to promote excited states generally involve a mixture of Metal to Ligand Charge Transfer (MLCT) and Ligand to Ligand Charge Transfer (LLCT), hence the energy gap HOMO-LUMO ($\Delta E_{H-L}$) modules the emission energy [13].

LUMO stabilization to decrease $\Delta E_{H-L}$, has been achieved with electron withdrawing N^N ligands by the incorporation of acceptor substituents such as acids or esters, as well as through the inclusion of highly conjugated systems [14]. For example, the $[Ir(ppz)_2(CO_2Et\text{-}bpy)]+$, complex (ppz: 1´-phenylpyrazole and $CO_2$Et-bpy: 4,4'-bis(ethoxycarbonyl)-2,2'- bipyridine) showed emission at 628 nm in acetonitrile by the ester group effect compared than $[Ir(ppz)_2(bpy)]+$ complex ($\lambda_{em}$ = 563 nm) [15]. Another alternative has been the use of benzothiazole moieties that promote substantially red-shifted emissions, as was observed in an Ir(III) complex with 2,2′-bibenzo-[d]thiazole with emission at 686 nm in $CH_2Cl_2$ solution [16]. To obtain blue emissions, the most used strategy is the incorporation of electron withdrawing C^N ligands [17,18] as showed the $[Ir(F_2ppz)_2(t\text{-}butyl\text{-}bpy)]+$ complex ($\lambda_{em}$ = 495 nm) with respect to [Ir(ppz)2(t-butyl-bpy)]+ $\lambda_{em}$ = 555 nm) (t-butyl-bpy: 4,4´-di-tert- butyl-2,2´-bipyridine), where the presence of fluorine atoms promotes stabilization of HOMO increasing the emission energy [19]. The effect of fluoride substituents has also been observed in the $[Ir(F_2ppy)_2(tzpy\text{-}cn)]+$ ($F_2$ppy: 2-(2,4-difluorophenyl) pyridine and tzpy-cn: 2,2-dimethyl-6-(3-(pyridin-2-yl)-4H-1,2,4-triazol-4-yl) hexanenitrile)) complex with a vibronic structure emission with two peaks at 456 and 486 nm [20].

The increment of stable Ir-iTMCs with full-color emissions has been and will continue to be a challenge for lighting applications, being essential reduce costs in the synthesis of ligands, avoiding complicated synthetic steps that give low-yield products. Besides, with appropriate mixtures of iTMCs (Red, Green and Blue: RGB), it is possible to produce a white-light multicomponent LEC, where the great challenge is to achieve a wide band gap for blue iTMCs and stable red emitter complexes. In this sense, this article shows the rationalized synthesis, characterization and photophysical study of six Ir (III) complexes that display emission in a wide range. The understanding of electronic properties was complemented by theoretical studies through DFT calculations. The complexes studied (Figure 1) are: $[Ir(F_2ppy)_2(neo)](PF_6)$ (C1), $[Ir(F_2ppy)_2(biq)](PF_6)$ (C2), $[Ir(F_2ppy)_2(dabiq)](P_{F6})$ (C3), $[Ir(bzq)_2(neo)](PF_6)$ (C4), $[Ir(bzq)_2(biq)](PF_6)$ (C5), $[Ir(bzq)_2(dabiq)](PF_6)$ (C6), where C^N ligands are $F_2$ppy and bzq: benzoquinoline; and as N^N ligands were used neo: neocuprine, biq: biquinoline and dabiq: (2,2'-biquinoline)-4,4'-dicarboxylic acid. The C^N and N^N were selected to accomplish synergic effect in the electron-density distributions of excited states for each Ir-iTMC to contribute the diversification of the emission colors and/or possible blends to promote future white light emissions.

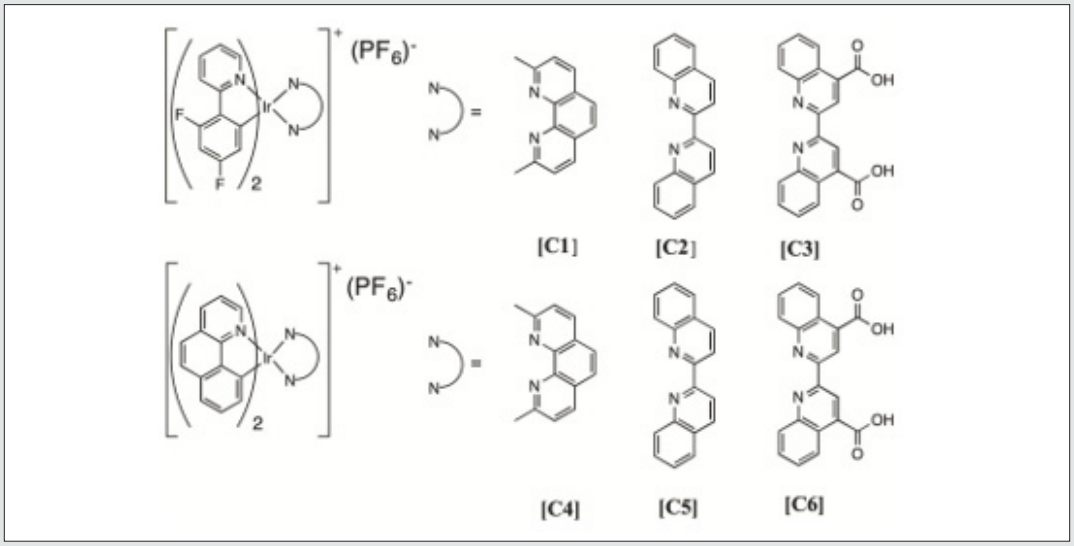


**Figure 1:** Chemical structure of cationic Ir (III) complexes C1-C6.

## Results and Discussion

### Experimental and theoretical structural characterization

The synthesized complexes were characterized by FT IR, MALDI-MS and $^1$H NMR spectroscopies (see Supporting Information, SI). C2, C4 and C5 complexes have been synthesized previously [21,22]. All FT IR spectra showed the characteristic $PF_6$- peaks ~ 845 and 559 $cm^{-1}$. [23-25] In addition, for C3 and C6 the peaks associate to vibrational modes of the acid substituents (C=O and O-H) were observed. [26] The characterization by $^1$H NMR spectroscopy confirmed the structures of the complexes from the signals with their corresponding multiplicities and integrations.

For C1 and C4 the singlet at 2.10 ppm (C1, DMSO-$d_6$) and 1.96 ppm (C4, $CDCl_3$) evidence the presence of the methyl protons; for C3 and C6 the signal at 8.89 ppm (DMSO-$d_6$) is attributed to the proton of the acid groups.

Besides, in C1, C2 and C3 the signals of the $H_5$ and $H_6$ show a splitting consistent with the proton-fluorine coupling, since the fluorine is an active nucleus in NMR.[14] Analogous Iridium (III) complexes with $F_2$ppy as cyclometalating ligand show a similar patter splitting [27,28]. The C1-C6 optimized molecular structures in the ground state ($S_0$) were calculated ($PF_6$- was not incorporated) and all the selected geometrical parameters are listed in the Supporting Information. All the complexes show a distorted octahedral coordination around the central metal. The bond lengths involving the metal center appear in the following ranges: Ir-$C_1$ = 2.02-2.03 Å (like Ir-$C_2$), Ir-$N_1$ = 2.08-2.10 Å (like Ir-$N_2$), Ir-$N_3$ = 2.30-2.33 Å (like Ir-$N_4$). The angles that involve the metal center appear in the following ranges: ∠$C_1$-Ir-$N_1$ = 94.61°-95.93°, ∠$N_3$-Ir-$N_4$ = 74.07°-74.57°, ∠$N_1$-Ir-$N_2$ = 173.91°- 174.95°, ∠$C_1$-Ir-$N_3$ = 175.58°-177.09°, and for the dihedral angles: ∠$N_3$-$C_3$-$C_4$-$N_4$ = 1.29°- 25.87°, ∠$C_1$-$C_2$-$N_3$-$N_4$ = 2.99°-6.03°, ∠$C_2$-$N_1$-$N_4$-$N_2$ =4.73°-5.90°. In general, no significant differences were found between the studied complexes and the parameters agree with the structures of analogous Ir (III) complexes. However, some differences are observed in ∠$N_3$-$C_3$-$C_4$-$N_4$ dihedral angle where for C1 and C4 this angle is smaller respect to the other complexes (1.9 and 1.3° for C1 and C4, respectively, vs 24-26° in the remaining complexes) which indicates a higher planarity degree of neo ligand in comparison to biq and dabiq ligands. Moreover, in ∠$C_1$-$C_2$-$N_3$-$N_4$ dihedral angle highest values are observed for C1 y C4, which is attributed to the presence of the methyl substituents in the positions 6 and 6´of phenanthroline skeleton that induce steric hindrance, locating this ligand out of the plane to favor a suitable spatial arrangement of the atoms in the complexes.

## Electrochemical properties

The cyclic voltammograms (CV) of the complexes were recorded in acetonitrile solutions using Ag/AgCl as reference electrode (see SI). The assignments of the reduction and oxidation processes were carried out by comparing to electrochemical data reported for similar cyclometalated Ir (III) complexes. [29-31] The values of the redox potentials are shown in Table 1. Towards positive potentials the redox process of $Ir^{(4+/3+)}$ couple is registered [32]. These processes also have contributions associated to cyclometalating ligands in agree with the values for C1, C2 and C3 (1.72 V, 1.70 V and 1.88 V, respectively), which are similar among them due to the presence of $F_2$ppy; as it also happens with C4, C5 and C6 (1.30 V, 1.31 V and 1.46 V, respectively) that contain bzq. The oxidation processes of $F_2$ppy-complexes are at higher potentials than bzq-complexes, as expected due to the electron-withdrawing nature of $F_2$ppy ligand, which promotes the oxidation of the metallic center at higher energy [33]. Furthermore, the influence of the ancillary ligands on oxidation is strong for C3 and C6 complexes, due to the acceptor character of the dabiq ligand given by the acid substituents. Similar behavior has been observed in Ru-bpy complexes with and without ester group, where the oxidation of Ru-bpy complex is at 1.29 V and for Ru-bpy-ester complex at 1.55 V [34].

**Table 1:** Values of the redox processes for complexes C1–C6.

| Complex | $E_{ox}$ ($Ir^{4+/3+}$)/V[a] | $E_{red}$ ($L/L^-$)/V[a] | $\Delta E_{red-ox}$/V[b] | $\Delta E_{HL}$/eV[c] |
|---|---|---|---|---|
| C1 | 1.72 | -1.35 | 3.07 | 3.29 |
| C2 | 1.7 | -0.85 | 2.55 | 2.95 |
| C3 | 1.88 | -0.56 | 2.44 | 2.65 |
| C4 | 1.3 | -1.41 | 2.71 | 2.99 |
| C5 | 1.31 | -0.87 | 2.18 | 2.67 |
| C6 | 1.46 | -0.76 | 2.22 | 2.36 |

[a]$E_{ox}$ ($Ir^{4+/3+}$) and $E_{red}(L/L^-) = 1/2(E_{pa} + E_{pc})$; L is referred to N^N ligand; acetonitrile/$TBAPF_6$ 0.1 M, vs. Ag/AgCl. [b]$\Delta E_{red-ox} = E_{ox}$ ($Ir^{4+/3+}$) - $E_{red}(L/L^-)$. [c]$\Delta E_{HL}$, H = HOMO and L = LUMO, data from theoretical calculations.

At negative potentials the complexes show a redox process assigned to a reduction on the N^N ligand, [35] evidenced by the similar values in the C1/C4, C2/C5 and C3/C6 complex pairs. The more negative values for this reduction are assigned to the complexes with neo ligand (C1 and C4) since this ligand has an electron-donor character in comparison with biq and dabiq. Here, the methyl substituents confer the donor character, as have been identified in more negative reduction potentials of Ir (III) complexes with bipyridine or phenanthroline with presence of methyl substituents in comparison to the reductions of their analogous complexes without methyl substituents [36]. Conversely, between C2/C5 and C3/C6 pairs, the complexes with acid group (dabiq) show less negative reduction due to the higher acceptor character of dabiq given by electron withdrawing substituents in 4 and 4´positions [37]. Since the oxidation and reduction potentials are related to HOMO and LUMO frontier orbitals, we estimated $\Delta E_{HL}$ from the potentials ($\Delta E_{red-ox}$), which values follow a decreasing trend as: C1 > C4 > C2 > C3 > C6 > C5. This tendency shows that the highest gaps of C1 and C4 could be yield the complexes with emissions at higher energy compared to C6 and C5 with emissions probably shifted to red. Relate to theoretical studies, the energies of the molecular orbitals were calculated for all complexes. Fig. 2 shows the energy diagram and density surfaces of HOMO and LUMO frontier molecular orbitals, while the molecular orbital energies and compositions are tabulated in the Supporting Information, from HOMO-2 to LUMO+2. In all cases HOMO orbitals are composed

by a mixture of π and d orbitals of the cyclometalating ligand (63-70%) and metal (28-35%), respectively. For LUMOs, the electron density is mainly delocalized on the ancillary ligand (~96%). These electronic distributions agree with the metal oxidation and N^N ligand reductions described by CV. The HOMOs-1 and HOMOs- 2 orbitals are mainly composed C^N ligand orbitals (~96% and 77%, respectively), below from HOMOs in around 0.2-0.3 eV and 0.4-0.6 eV, respectively. In the case of LUMOs+1, the composition is centered in the orbitals of the N^N ligands (~96%) and they are above to LUMOs in around 0.3-0.9 eV; the LUMOs+2 is largely composed by orbitals of the C^N ligands (~90%) and they are above to LUMOs ~ 0.6-1.5 eV. The most stabilized HOMO orbitals are in C1-C3 series (0.50-0.53 eV lower than C4-C5 series) due to the fluoride substituents of the C^N ligand, in contrast to C4-C6 that contain bzq. For LUMOs, C1 and C4 have energies ~ 0.30 eV higher than C2 and C5, and the energies of these latter are ~ 0.40 eV higher than C3 and C6. These tendency evidence the increment of the electron withdrawing character of the N^N ligands in the order dabiq > biq > neo, as it was also described by CV experiments. The theoretical $\Delta E_{HL}$ were determined and the values are listed in Table 1. A comparison of the theoretical and experimental results ($\Delta E_{HL}$ vs $\Delta E_{red\text{-}ox}$) shows the same tendency; however, some discrepancies can be observed for C5, which could be ascribed to possible electrochemical adsorption/desorption processes of the electroactive species onto electrode surface [38].

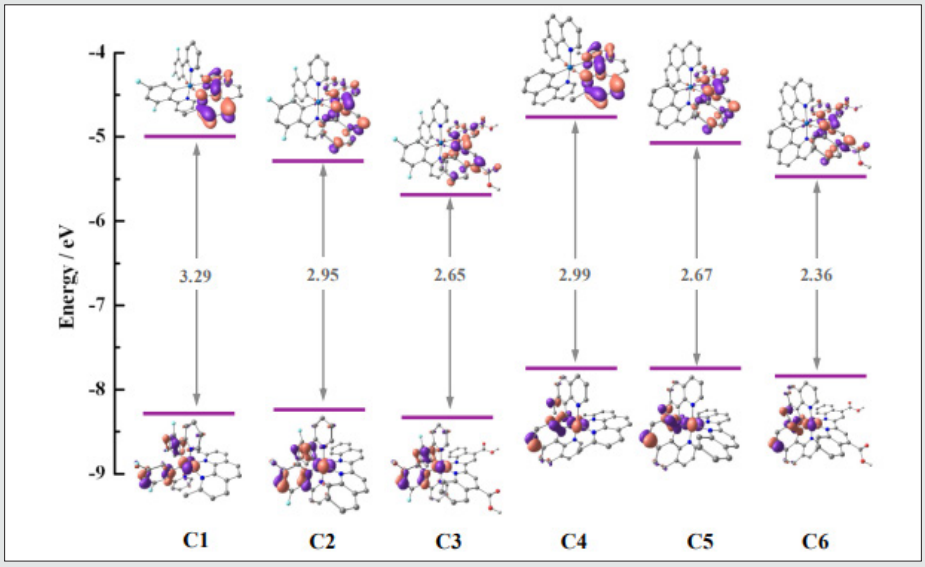


**Figure 2:** Energy diagram and isosurfaces of HOMO and LUMO for C1-C6.

## Charge injection and transport properties

The balance between injection/transport of holes and electrons is decisive for an iTMC can be used in LEC devices, since this balance determines the luminance, turn-on time, and lifetime of the device [39]. The energy barrier for the injection of holes and electrons, is related to the ionization potential (IP) and electronic affinity (EA) [40]. Here, these thermodynamic parameters were calculated and analysed respect to the energies of the frontier orbitals. These parameters are defined as: $IP = E_{N-1} - E_N$ and $EA = EN - E_{N+1}$, where EN, $E_{N+1}$, and $E_{N-1}$ correspond to the total energies of the molecular system in its fundamental state (EN) and with one more electron ($E_{N+1}$) and one less electron ($E_{N-1}$) [41,42]. To identify a favored hole injection from the anode into the iTMC are expected low IP values; conversely, for an efficient electron injection from the cathode into the iTMC, high EA values are expected [43] Considering the MLCT and LLCT are the main electronic transitions involved in the radiative decay, the HOMO should be correlated with IP since in this orbital the holes are formed, namely, in the metal and C^N ligand orbitals. Table 2 shows the IPs calculated for the complexes where the lowest values are in the complexes with bzq as cyclometalating ligand (C4, C5 and C6), therefore, in these complexes the hole injection should be easier compared to complexes with $F_2$ppy. The IP values agree with the highest HOMOs determined by the theoretical calculations and predicted by CV. This trend is in concordance with electron donor nature of bzq that promote the HOMO destabilization.

In the LUMO the electron arrives, residing primarily in the ancillary ligand, therefore, the energy of this orbital is correlated with the EA. The data of Table 2 show the highest EA values to C3 and C6, intermedia for C2 and C5 and the lowest are found to C1 and C4, following an order relate to ancillary ligand as: *C-dabiq > C-biq > C-neo*. These electronic affinities agree with the LUMO energies determined both theoretical calculations and predicted by CV and indicate the complexes with highest EA have the lowest energy barrier for electron injection. The trend follows the regimen from an electron acceptor for dabiq to an electron donor in neo, where these extreme ligands promoting stabilization and destabilization of LUMO, respectively. The reorganization energies of hole and electron ($\lambda_{hole}$ and $\lambda_{electron}$) are the kinetic parameters that determine the transport balance between holes and electrons [26] The reorganization energy relates to charge transfer rate as follow: k

= $A_{exp}(-\lambda/k_BT)$, where A is the electronic coupling factor, kB is the Boltzmann constant, and T is temperature. The reorganization energies are determined according to: $\lambda_{hole}$ = IP−HEP and $\lambda_{electron}$ = EA−EEP, where HEP and EEP correspond to the hole and electron extraction potentials, respectively, which are calculated as the vertical energy difference between the relaxed cationic (anionic) molecule and the neutral molecule at the cationic (anionic) geometry [44-46]. An efficient charge transport process relates with a low reorganization energy, then, as show the results in Table 2, the $\lambda_{electron}$ are lower compare to $\lambda_{hole}$, therefore, the performance of these complexes are optimized to electron transport than for hole transport.[47] However, the complexes with $F_2$ppy have similar values 0.38 eV and all the complexes with bzq have 0.35 eV, indicating that in the triad of C4, C5 and C6 the transport of hole is slightly favored compare to the other complexes. In the case of $\lambda_{electron}$, the tendency of values is related to the nature of ancillary ligand, where the lowest values are obtained with the C-neo, intermedia with C-biq and highest with C-dabiq. Therefore, in C1 and C4 it could be considered that the electron transport is favored compared to the other complexes. Besides, the energy difference between $\lambda_{hole}$ and $\lambda_{electron}$ ($\Delta\lambda$) are smaller in all systems ranged between 0.03-0.12 eV. These values indicate hole and electron transfer balance could be achieved easily in emitting layer. For example, an analogous Ir (III) complex exhibit a maximum luminance of 177 cd/m$^2$ and was characterized by a $\Delta\lambda$ = 0.20, therefore, it is expecting the complexes studied as suitable iTMCs for LEC applications.

**Table 2:** Transport and injection electronic parameters for C1-C6. Ionization potential (IP), electron affinity (EA), and recombination energies ($\lambda_{hole}$ and $\lambda_{electron}$) in eV.

| Complex | IP | EA | $l_{hole}$ | $l_{electron}$ | Dl |
|---|---|---|---|---|---|
| C1 | 4.43 | 3.92 | 0.37 | 0.25 | 0.12 |
| C2 | 4.5 | 4.4 | 0.38 | 0.28 | 0.1 |
| C3 | 4.42 | 5.05 | 0.38 | 0.32 | 0.06 |
| C4 | 4.14 | 3.77 | 0.35 | 0.24 | 0.11 |
| C5 | 4.22 | 4.26 | 0.35 | 0.28 | 0.07 |
| C6 | 4.13 | 4.93 | 0.35 | 0.32 | 0.03 |

## UV-Vis absorption properties

The absorption spectra of complexes were registered in acetonitrile solutions and are show in Figure 3A. The wavelengths of electronic transitions involved in the emission processes and the corresponding molar absorptivity coefficients are summarized in (Table 3) fig 3. The absorptions at high energies (220-280 nm) are assigned to the spin-allowed ligand-centered ($^1$LC) $\pi \rightarrow \pi^*$ transitions that involved both ancillary and cyclometalating ligands [48, 49, 50]. The bands observed between 340-400 nm can be ascribed at the first glance to $^1$MLCT and $^1$LLCT, where $^1$MLCT involves an electronic density transition from metal to ancillary ligand, meanwhile, $^1$LLCT involves a transition from the cyclometalating ligand (phenyl fragment) to the ancillary ligand [51, 52, 53]. The absorptions observed higher than 400 nm are attributed to spin-forbidden transitions towards triple states, which are enabled by the high spin–orbit coupling of the Iridium [54, 55, 56]. To understand the nature of the electronic transitions, the theoretical absorption spectra based on the optimized geometry of the ground states were determined by TD-DFT methodology, focusing on the transitions between 340 to 400 nm which are related to the photophysical properties of these complexes. The vertical electronic excitation energies, the oscillator strengths, the mono excitations, and the nature of the excited states were determined and listed in the Supporting Information.

**Table 3:** Photophysical properties of C1-C6 complexes in acetonitrile solution.

| Complex | $\lambda_{abs}$/nm (ε/M$^{-1}$cm$^{-1}$) | $\lambda_{em}$/nm | $\Phi_{em}$/% | τ/μs | $k_r/10^5$ | $k_{nr}/10^5$ |
|---|---|---|---|---|---|---|
| C1 | 361 (9120) | 490 | 43 | 2.34 | 1.84 | 2.43 |
| C2 | 370 (9280) | 585 | 27 | 1.62 | 1.67 | 4.5 |
| C3 | 373 (10070) | 580 | 11 | 2.47 | 0.45 | 3.6 |
| C4 | 364 (10550) | 515 | 20 | 3.23 | 0.62 | 2.48 |
| C5 | 371 (9520) | 617 | 3 | 2.78 | 0.11 | 3.49 |
| C6 | 372 (10790) | 605 | 5 | 1.25 | 0.4 | 7.6 |

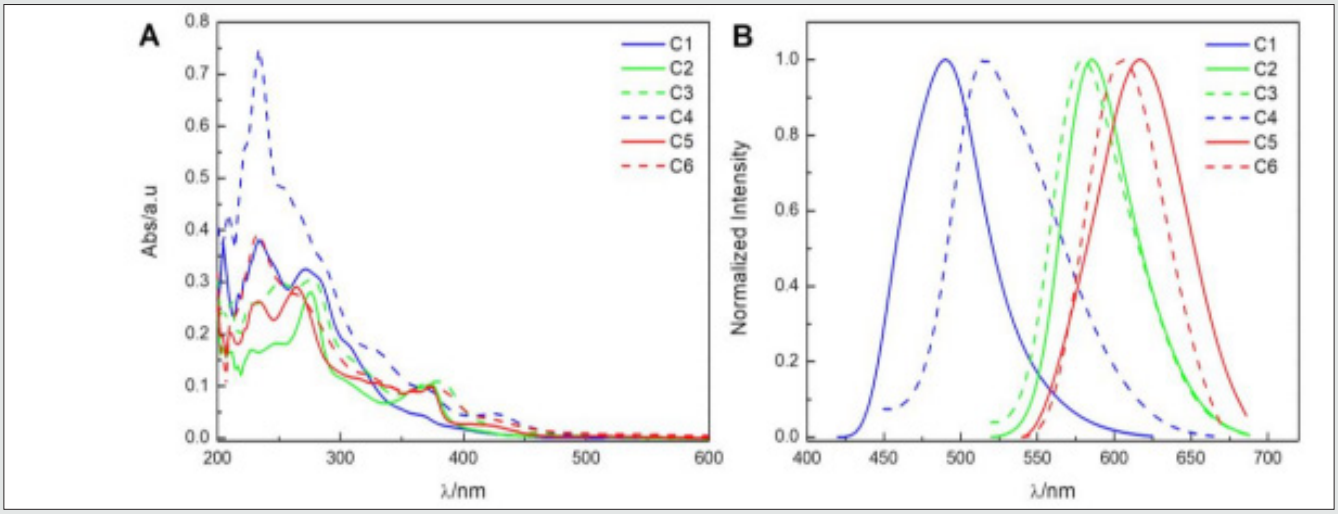


**Figure 3:** Absorption spectra of C1-C6 at $10^{-5}$ M. B. Normalized emission spectra of C1-C6. Both spectra registered in acetonitrile solutions.

For C1 three states are associated with the absorption band ~ 360 nm: $S_3$, $S_6$ and $S_7$ corresponding to transitions from H → L+2, H-1 → L and H-3 → L, respectively, giving a mixture of $^1$MLCT/$^1$LLCT/$^1$LC characters. In the case of C2, the $S_4$ and $S_6$ states would be responsible for the broad absorption band located at 370 nm, originated from the H-4 → L and H → L+2 transitions, respectively, corresponding to a mixture of $^1$MLCT/$^1$LC characters. In C3, two states are related with the absorption at 373 nm: $S_5$ and $S_6$, due to transitions from H-4 → L and H → L+1, respectively, giving a mixture of $_1$MLCT/$_1$LLCT characters. For C4, three excited states are involved to absorption at 364 nm: $S_3$, $S_4$ and $S_5$ states due to electron promotions from H → L+1, H-3 → L and H → L+2, respectively, showing a mixed of $_1$MLCT/$_1$LLCT/$_1$LC characters. In C5 three excited states ($S_4$, $S_5$ and $S_6$) were computed to explain the experimental band at low energy, that involve H → L+1, H-3 → L and H → L+2 ($^1$MLCT/$^1$LLCT/$^1$LC characters) transitions. Finally, C6 shows two transitions responsible of absorption at 372 nm ($S_8$ and $S_9$), due to transitions from H-5 → L and H → L+2 ($^1$MLCT/$^1$LC characters), respectively.

## Photoluminescence properties

The emission spectra registered in degassed acetonitrile solutions are shown in (Figure 3B). and the associated data are summarized in (Table 3). (Figure 3B). shows broad emission profiles attributable to radiative deactivations from the $^3$MLCT or $^3$LLCT excited states or a mixture of both, according with to the description of analogous Ir (III) complexes C1 and C4 show emissions towards higher energies in agreement with the electro-donor nature of the neo ligand. Since C1 has an electron withdrawing ($F_2$ppy) cyclometalating ligand their emission is blue shifted compared to C4. This same dependence is observed comparing C2 and C3 with C5 and C6, respectively. Therefore, $F_2$ppy favored the HOMO stabilization allowing an increment of HOMO–LUMO gap, [57] which is in good agree with the theoretical calculations see (Figure 2). The emission at intermediate energies is observed for C2 and C3, and towards to the red for C5 and C6. Since dabiq is the N^N ligand with the stronger acceptor character, it expected that the complexes C3 and C6 show emissions most red-shifted, however, it is possible to note the C3 emission slightly blue shifted compared to C2 (similarly in C6 respect to C5). This behavior could be attributed to geometrical distortions as it evidenced by the highest $C_1$-$C_2$-$N_3$-$N_4$ and $C_2$-$N_1$-$N_4$-$N_2$ dihedral angles for C3 compared to C2, promoting an emission energy increase, as it also has been described for analogous complexes [58].

On the other hand, the relative emission quantum yields were determined showing the highest values for C1 and C4, and the lowest for C5 and C6 in agreement with the "energy gap law" [59] The decay of the emission process was monitored by time-resolved emission experiments at room temperature in both air-equilibrated and degassed acetonitrile solutions. In degassed solutions, all the studied complexes exhibited a single-exponential decay with lifetimes between 1.25-3.23 μs, typically of phosphorescence [60,61]. In air-equilibrated solutions, all lifetimes were lower than those registered at $N_2$ atmosphere (between 90-560 ns, see SI), evidencing the phosphorescence for the studied complexes [62]. The radiative and non-radiative rate constants were estimated from the emission lifetimes and quantum yields values. As expected, the complexes that show higher emission quantum yields are those with higher radiate rate constants ($k_r$) values, while C6 has the highest non-radiative rate constant, in agreement to their low quantum yield. To gain further insight of the nature of the state responsible for the emission, the optimized structures of the lowest triplet states ($T_1$ for C1, C2, C4 and C5; $T_3$ for C3) were determined (the geometric parameters are reported in the SI). For C6, it was not possible to find a triplet excited state coherent with the experimental emission value. For all complexes, the structures of the triplet states show shorter bond lengths than in the ground

state, except for Ir-$N_1$ and Ir-$N_2$ bonds, which practically show no variation. The decrease in Ir-$N_3$ (and Ir-$N_4$) bond length suggests that the metal-ligand bond is strengthened, which could facilitate the metal to ligand charge transfer transition [63]. The dihedral angles that contain the metal center show the distortion of the octahedral geometry, like occur in the ground states.

The theoretical phosphorescence energies in acetonitrile were determined considering the vertical energy difference between the relaxed triplet state and the ground state at the triplet state geometry. The emission energies obtained from $T_1$ states were: 2.54 eV (490 nm), 2.20 eV (562), 2.30 eV (540 nm) and 1.94 (640 nm) for the complexes C1, C2, C4 and C5, respectively, which agree with the experimental energies. The electronic transitions responsible for radiative deactivation pathways of the emitting states are composed by $^3$MLCT and $^3$LLCT characters [N^N(π*) → Ir(d) + C^N(π)] as it observed from Hole (blue) and electron (violet) distributions with the main pair-orbital contributions for the deactivation of the first triplet excited state (T1) for complexes C1, C2, C4, C5 and third triplet excited state (T3) for C3, corroborating that these radiative deactivations are mainly associated with the LUMO → HOMO transition (over 90%). On the other hand, the emitting state determined for C3 is $T_3$, since the calculated energy of this state (1.91 eV, 649 nm) is the closest related to the experimental value (580 nm). Similar differences between theoretical and experimental energies have been described for other complexes of Ir(III). The $T_1$ and $T_2$ states are discarded as emitters because the calculated energies in both cases are at least 192 nm above the experimental emission wavelength. For C3, the emissive triplet is described as a mixture of $^3$MLCT/$^3$LC characters [N^N($\pi^*$) → Ir(d) + N^N(π)] (Figure 4) and its radiative deactivation is mainly due the transition LUMO → HOMO-5 (42%)

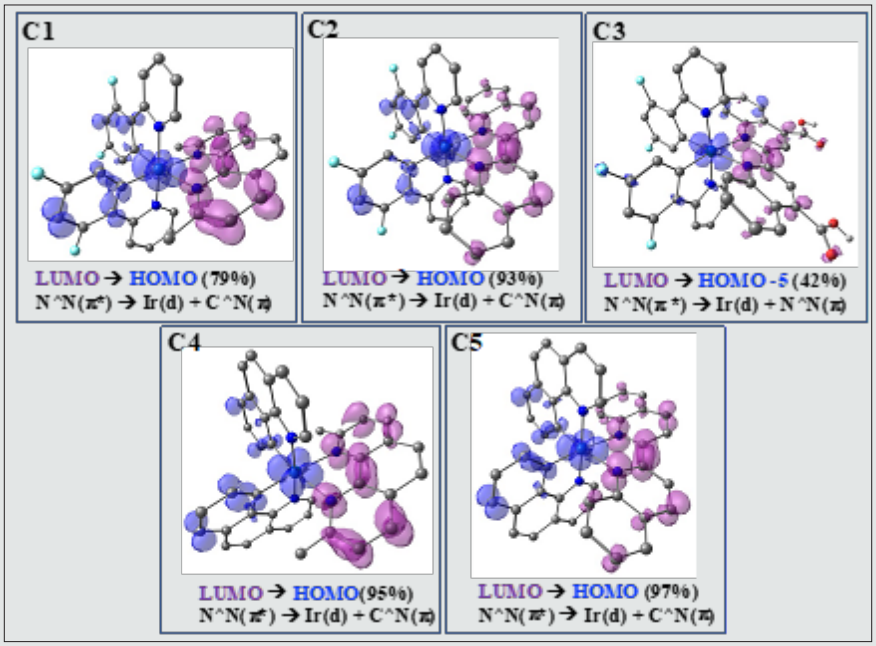


**Figure 4:** Hole (blue) and electron (violet) distributions with the main pair-orbital contributions for the deactivation of the first triplet excited state (T1) for complexes C1, C2, C4, C5 and third triplet excited state (T3) for C3.

## Energies offset diagrams in host-guest systems

The stable and pure white light emission from the LEC devices have been commonly achieved with the host–guest strategy, since a single luminescent iTMC cannot cover enough spectral width to produce white emission [64]. With this strategy a blend of two or three emissive molecules that comprise a high-gap host (blue or blue-green emitters) and low-gap guests [65]. In addition, the offsets in energy levels of host and guest iTMCs should be considered to promote a suitable carrier balance, favoring the emission zone near the center of the emissive layer, avoiding exciton quenching, therefore, improving device efficiency [66].

Considering the photophysical and electrochemical properties of C1-C6 iTMCs evaluated in this work, we propose suitable blends to produce host-guest systems as potential white LECs, Fig. 5. Energy levels derived from the CV data of: A.) hostguest single-doped system with C1 and C6, B) host-guest double-doped system with C1,C2 and C6. ITO and Al represent anode and cathode, respectively. The first proposal is a single-doped host-guest system (Figure 5A) involved C1 as host doped with C6 as guest. In this system the requirements of blue host doped with a red iTMC is satisfied, compared for example with a white LEC composed with emitters at 513 and 591 in acetonitrile solutions (499 and 607 in film), yielding CIE coordinates in the white region (0.42, 0.41) with a maxima Luminance of 42.5 cd/m$^2$ at bias 3.5 V [67]. In the proposal system the energy offset of host-guest at LUMO levels is 0.59 eV and HOMO levels it is 0.26 eV. This tendency probably will produce an electron trapping (hole injection favored over

electron injection), which could be avoiding by modulation of the bias applied and/or host-guest concentrations. [68,69] Another alternative is a double-doped host-guest system as show Figure 5B. Here, also C1 is proposed as host double doped with C2 and C6, where due to the presence of C2, the LUMO and HOMO gaps are reduced between the blue and red emitters, allowing an improved carrier balance to compare the single host-guest system.

This proposal is comparable with a previously described double doped host-guest device with blue, orange, and red emitters, yielding a white LEC (0.32, 0.43 CIE coordinates) with 20.2 cd/m$^2$ of maxima luminance at 3.3 V.[38b] In this way, we can project in a rational way and based on the electronic studies of our systems, two forms of possible white LECs with two or three cyclometalated Ir (III) complexes of easy synthesis.

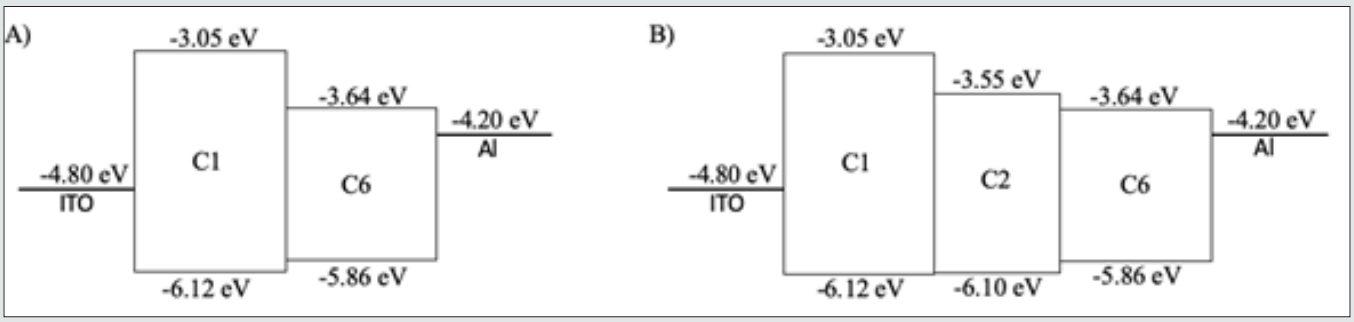


**Figure 5:** Energy levels derived from the CV data of: A.) host-guest single-doped system with C1 and C6, B) host-guest double-doped system with C1, C2 and C6. ITO and Al represent anode and cathode, respectively.

## Conclusions

The Ir (III) complexes studied are suitable as luminescent materials for LEC applications, allowing to increase the number of iTMC that can produce emission at wide range of colors. The modulation of emission energy was achieved successfully by a selection of commercial ancillary and cyclometalating ligands, avoiding the reactions of complicated ligands that obviously affect the yield in the synthesis of an iTMC. According to the experimental and theoretical results, C1 complex is proposed as new efficient blue emitter for LEC devices since their $F_2$ppy ligands promote a strong stabilization of HOMO, increasing the emitting state energy. Considering the high demand of stable blue- iTMC, C1 stands out by their high quantum yield, from an excited state with $^3$MLCT and $^3$LLCT characters (95% of LUMO → HOMO transition). The C4 complex show emission at 515 nm with a proper quantum yield, and C2 and C3 are emitters around 580 nm that can be useful in blends for double doped host-guest systems. C5 and C6 complexes depicted emissions at lower energies but with lower quantum yield, however, these red emitters displayed surprising electron injection and transport properties, highlighting the high values of electronic affinities. In addition, this study shows valuable precedents to continue exploiting these complexes, optimizing their LEC performances with both single luminescent iTMCs and to produce white light from host- guest systems.

## Acknowledgements

This work was supported by FONDECYT project N°1201173 and PI_M_2020_31 USM project. D. F. acknowledges to CONICYT through their FONDECYT research program (1160443) for the acquisition of the Lifespec II spectrometer. I. G acknowledges to FONDECYT 11180185, M. S-N. acknowledges to FONDECYT 3170663, F. S. acknowledges to the CONICYT-ANID PhD scholarship and J. M. acknowledges to FONDECYT 1180673 and Office of Naval Research grant N°62909-18-1-2180.

## References

1. Hu T, a) T. Hu, L. He, L. Duan, Y. Qiu, J. Mater. Chem. 2012, 22, 4206-4215; b) J. Slinker, J.Defranco, M. Jaquith, W. Silveira, Y. Zhong, J. Moran-Mirabal, H. Craighead, H. Abruna, J.Marohn, G. Malliaras, Nature. Mater. 2007, 6, 894-899; c) H. Su, Y. Chen, K. Wong, Adv.Funt. Mater. 2019, 1906898.
2. Slinker J, Defranco J, Jaquith M, Silveira W, Zhong Y, et al. (2007) Direct measurement of the electric- field distribution in a light-emitting electrochemical cell. Nature Material 6: 894-899.
3. Su H, Chen Y, Wong K (2019) Recent Progress in White Light-Emitting Electrochemical Cells. Adv Funt Mater 30(33): 1906898.
4. Dias F, Bourdakos K, Jankus V, Moss K, Kamtekar K, et al. (2013) Triplet harvesting with 100% efficiency by way of thermally activated delayed fluorescence in charge transfer OLED emitters. Adv Mater 25(27): 3707-3714.
5. Reineke S, Lindner F, Schwartz G, Seidler N, Walzer K, et al. (2009) White organic light-emitting diodes with fluorescent tube efficiency. Nature 459(7244): 234-238.
6. Costa RD, Orti E, Bolink HJ, Monti F, Accorsi G, et al. (2012) Luminescent ionic transition-metal complexes for light-emitting electrochemical cells. Chem Int Ed 51(33): 8178-8211.
7. Xu L, Yuan S, Zeng H, Song J (2019) A comprehensive review of doping in perovskite nanocrystals/quantum dots: evolution of structure, electronics, optics, and light-emitting diodes. Mater Today Nano 6: 100036.
8. Lee J, Yoo D, Handy E, Rubner M (1996) Thin film light emitting devices from an electroluminescent ruthenium complex. Appl Phys Lett 69(12): 1686-1688.

9. Pei Q, Yu G, Zhang C, Yang Y, Heeger A, et al. (1995) Polymer light-emitting electrochemical cells. Science 269(5227): 1086-1088.

10. Sandström A, Edman L (2015) Towards High-Throughput Coating and Printing of Light-Emitting Electrochemical Cells: A Review and Cost Analysis of Current and Future Methods 3(4): 329-339.

11. Slinker J, Rivnay J, Moskowitz J, Parker J, Bernhard S, et al. (2011) Pure Appl Chem 83: 2115-2128.

12. S van Reenen, P Matyba, A Dzwilewski, R Janssen, L Edman, et al. (2010) J Am Chem Soc 132: 13776-13781.

13. Zhao J, Chi Z, Yang Z, Chen X, Arnold M, et al. (2018) Recent developments of truly stretchable thin film electronic and optoelectronic devices. Nanoscale 10(13): 5764-5792.

14. Namanga JE, Gerlitzki N, Mallick B, Mudring A (2017) Long term stable deep red light-emitting electrochemical cells based on an emissive, rigid cationic Ir(iii) complex. J Mater Chem C5(12): 3049-3055.

15. Kaihovirta N, Longo G, Gil-Escrig L, Bolink HJ, Edman L, et al. (2015) Self-absorption in a light-emitting electrochemical cell based on an ionic transition metal complex. Appl Phys Lett 106(10): 103502.

16. González I, Gómez J, Santander-Nelli M, Natali M, Cortés-Arriagada D, et al. (2020) Synthesis and photophysical characterization of novel Ir (III) complexes with a dipyridophenazine analogue (ppdh) as ancillary ligand. Polyhedron 186: 114621.

17. Ma D, Tsuboi T, Qiu Y, Duan L (2017) Recent Progress in Ionic Iridium (III) Complexes for Organic Electronic Devices. Adv Mater 29(3): 1603253.

18. Cortés- Arriagada D, Dreyse P, Salas F, González I (2018) nsights into the luminescent properties of anionic cyclometalated iridium (III) complexes with ligands derived from natural products. Int J Quantum Chem 118(17): e25664.

19. Lee S, Han W (2020) Cyclometalated Ir(iii) complexes towards blue-emissive dopant for organic light-emitting diodes: fundamentals of photophysics and designing strategies. Inorganic Chem Front 7: 2396-2422.

20. Martínez-Alonso M, Cerdá J, Momblona C, Pertegás A, Junquera-Hernández JM, et al. (2017) Highly Stable and Efficient Light-Emitting Electrochemical Cells Based on Cationic Iridium Complexes Bearing Arylazole Ancillary Ligands. Inorganic Chemistry 56(17): 10298-10310.

21. Suhr K, Bastatas L, Shen Y, Mitchell L, Holliday B, et al. (2016) ACS Appl Mater Interfaces 8(14): 8888-8892.

22. Housecroft C, Constable E Coor (2017) 350, 155-177.

23. Cortés-Arriagada D, Sanhueza L, González I, Dreyse P, Toro-Labbé A, et al. (2016) About the electronic and photophysical properties of iridium(iii)-pyrazino[2,3-f][1,10]-phenanthroline based complexes for use in electroluminescent devices. Phys Chem Chem Phys 2016, 18(2): 726-734.

24. Tamayo A, Garon S, Sajoto T, P Djurovich, I Tsyba, et al. (2005) Cationic bis-cyclometalated iridium (III) diimine complexes and their use in efficient blue, green, and red electroluminescent devices. Inorg Chem 44(24): 8723-8732.

25. He L, Qiao J, Duan L, Dong G, Zhang D, et al. (2009) Blue Green to Red Emitting Cationic Iridium Complexes with Imidazole-Type Ancilllary Ligands. Adv Funct Mater 19: 2950-2960.

26. González I, Cortés-Arriagada D, Dreyse P, Sanhueza-Vega L, Ledoux-Rak I (2015) Eur J Inorg Chem 29: 4946-4955.

27. González I, Dreyse P, Cortés-Arriagada D, Sundararajan M, Morgado C (2019) 48: 16459- 16459.

28. Li X, Minaev B, Ågren H, Tian H (2011) Theoretical Study of Phosphorescence of Iridium Complexes with Fluorine-Substituted Phenylpyridine Ligands. Eur J Inorg Chem 16: 2517-2524.

29. González I, Natali M, Cabrera A, Loeb B, Maze J, et al. (2018) Heteroleptic Cu(I) complexes bearing methoxycarbonyl-imidoylindazole and POP ligands - An experimental and theoretical study of their photophysical properties. New J Chem 42(15): 6644-6654.

30. Chen B, Li Y, Chu Y, Zheng A, Feng J, et al. (2013) Highly Efficient solid state white light-emitting Electrochemical cell: Highly efficient single-layer organic light-emitting devices using cationic iridium complex as host. Org Electron 14: 744-753.

31. Sauvageot E, Lafite P, Duverger E, Marion R, Hamel M, et al. (2016) Iridium complexes inhibit tumor necrosis factor-α by utilizing light and mixed ligands. J Organomet. Chem 808: 122-127.

32. Zhao Q, Yu M, Shi L, Liu S, Li C, et al. (2010) Cationic Iridium (III) Complexes with Tunable Emission Color as Phosphorescent Dyes for Live Cell Imaging. Organometallics 29(5): 1085-1091.

33. Socrates G (2004) Infrared and Raman characteristic group frequencies In: (Eds) tables and charts, John Wiley & Sons PP. 364.

34. Aguilar J, Morris G, Kenwright A (2014) "Pure shift" $^{1}$H NMR, a robust method for revealing heteronuclear couplings in complex spectra. RSC Adv 4(16): 8278-8282.

35. Schaefer T, Danyluk S, Bell C (1969) Signs of proton-proton and proton-fluorine spin-spin coupling constants in 2-fluoro-3-methylpyridine. Sigma and pi contributions to coupling in a nitrogen heterocycle Can J Chem 47: 1507-1514.

36. Dreyse P, González I, Cortés-Arriagada D, Ramírez O, Salas I, et al. (2016) New J Chem 40: 6253-6263.

37. Monti F, Baschieri A, Gualandi I, Serrano-Pérez J, Junquera-Hernández J, et al. (2014) ridium (III) Complexes with Phenyl-tetrazoles as Cyclometalating Ligands. Inorg Chem 53(14): 7709-7721.

38. Bünzli A, Constable E, Housecroft C, Prescimone A, Zampese J, et al. (2015) Exceptionally long-lived light-emitting electrochemical cells: multiple intra-cation π-stacking interactions in [Ir $(C^N)_2(N^N)$] $[PF_6]$ emitters Chem Sci 6: 2843-2852.

39. Tordera D, Delgado M, Ortí E, Bolink HJ, Frey J, et al. (2012) Stable Green Electroluminescence from an Iridium Tris-Heteroleptic Ionic Complex. Chem Mater 24(10): 1896-1903.

40. Anderson P, Keene F, Meyer T, Moss J, Strouse G, et al. (2002) Manipulating the properties of MLCT excited states. Dalton Trans 12: 3820-3831.

41. Ertl C, Momblona C, Pertegás A, Junquera-Hernandez J, La-Placa M, et al. (2017) Highly Stable Red-Light-Emitting Electrochemical Cells. J Am Chem Soc 139(8): 3237-3248.

42. Costa R, Ortí E, Tordera D, Pertegás A, Bolink H, et al. (2011) Stable and Efficient Solid-State Light-Emitting Electrochemical Cells Based on a Series of Hydrophobic Iridium Complexes. Adv Energy Mater 1(2): 282-290.

43. Srinivas K, Yesudas K, Bhanuprakash K, Rao V, Giribabu L, et al. (2009) A Combined Experimental and Computational Investigation of Anthracene Based Sensitizers for DSSC: Comparison of Cyanoacrylic and Malonic Acid Electron Withdrawing Groups Binding onto the TiO2 Anatase (101) Surface. J Phys Chem C 113(46): 20117-20126.

44. Bard A, Faulkner L (2001) Electrochemical Methods: Fundamentals and Applications; 2nd Eds John Wiley &amp, Sons, New York, USA pp. 864.

45. Bünzli A, Bolink H, Constable E, Housecroft C, Junquera-Hernández J, et al. (2014) Thienylpyridine-based cyclometallated iridium (III) complexes and their use in solid state light-emitting electrochemical cells. Dalton Trans 43(2): 738-750.

46. Dreyse P, Santander-Nelli M, Zambrano D, Rosales L, Sanhueza L, et al. (2020) Electron-donor substituents on the dppz-based ligands to control luminescence from dark to bright emissive state in Ir (III) complexes. Int J Quantum Chem 120(12): e26167.

47. Shang X, Li Y, Zhan Q, Zhang G (2016) Theoretical investigation of photophysical properties for a series of iridium(iii) complexes with different substituted 2,5-diphenyl-1,3,4-oxadiazole. New J Chem 2016, 40(2): 1111-1117.

48. Han D, Zhao L, Pang C, Zhao H (2017) Polyhedron 126: 134-141.

49. Shang X, Han D, Zhan Q, Zhang G, Li D, et al. (2014) Coordination Chemistry of Disilylated Germylenes with Group 4 Metallocenes. Organometallics 33(11): 3300-3308.

50. Han D, Hao F, Tian J, Pang C, Li J, et al. (2015) J Lumin 159: 66-72.

51. Han D, Shang X, Zhao L, Sun X, Zhang G, et al. (2014) Theoretical study on the electronic structures and phosphorescent properties of a series of iridium (III) complexes with N^C^N-coordinating terdentate ligands. Mol Phys 112(13): 1824-1830.

52. Zhao J, Hu Y, Dong Y, Xia X, Chi H, et al. (2017) Novel bluish green benzimidazole-based iridium(iii) complexes for highly efficient phosphorescent organic light-emitting diodes. New J Chem 41(5): 1973-1979.

53. Marcantonio M Di, Namanga J, Smetana V, Gerlitzki N, Vollkommer F, et al. (2017) Green-yellow emitting hybrid light emitting electrochemical cell. J Mater Chem 5(46): 12062-12068.

54. Shavaleev N, Scopelliti R, Grätzel M, Nazeeruddin MK, Pertegás A, et al. (2013) Pulsed-current versus constant-voltage light-emitting electrochemical cells with trifluoromethyl-substituted cationic iridium(iii) complexes. J Mater Chem 1(11): 2241-2248.

55. You Y, Nam W (2012) Photofunctional triplet excited states of cyclometalated Ir (iii) complexes: beyond electroluminescence. Chem Soc Rev 41(21): 7061-7084.

56. Arias M, Concepción J, Crivelli I, Delgadillo A, Díaz R, et al. (2006) Chem Phys 326: 54-70.

57. Bernard J, Fleury L, Talon H, Orrit M (1993) Photon bunching in the fluorescence from single molecules: A probe for intersystem crossing. J Chem Phys 98(2): 850-859.

58. Hübner C, Renn A, Renge I, Wild U (2001) Direct observation of the triplet lifetime quenching of single dye molecules by molecular oxygen. J Chem Phys 2001, 115(21): 9619-9622.

59. Xie L, Bai F, Li W, Zhang Z, Zhang H, Phys Chem Chem Phys 2015, 17, 10014-10021.

60. Cheng C, Wang C, Cheng J, Chen H, Yeh Y, et al. (2015) A two-dimensionally microporous thiostannate with superior Cs+ and Sr2+ ion-exchange property. J Mater Chem C 3(10): 5665-5673.

61. Lenes M, Garcia-Belmonte G, Tordera D, Pertegás A, Bisquert J, et al. (2011) Operating Modes of Sandwiched Light-Emitting Electrochemical Cells. Adv Funct Mater 21(9): 1581-1586.

62. Su H, Hsu J (2015) Improving the carrier balance of light-emitting electrochemical cells based on ionic transition metal complexes. Dalton Trans 44(18): 8330-8345.

63. Fresta E, Weber M, Fernandez-Cestau J, Costa R (2019) White Light-Emitting Electrochemical Cells Based on Deep-Red Cu(I) Complexes. Adv Optical Mater 7(23): 1900830.

64. Shafiee, Salleh M, Yahaya M (2011) Determination of HOMO and LUMO of [6,6]-Phenyl C61-butyric Acid 3-ethylthiophene Ester and Poly (3-octyl-thiophene-2, 5-diyl) through Voltametry Characterization. Sains Malaysiana 40(2): 173-176.

65. Leonat L, Sbarcea G, Branzoi I (2013) Cyclic voltammetry for energy levels estimation of organic materials. UPB Scientific Bulletin. Series B: Chemistry and Materials Science 75(3): 111-118.

66. Zeng Q, Li F, Guo T, Shan G, Su Z, et al. (2017) Synthesis of red-emitting cationic Ir (III) complex and its application in white light-emitting electrochemical cells. Org Electron 42: 303-308.

67. Shan G, Li H, Zhu D, Su Z, Liao Y, et al. (2012) Intramolecular π-stacking in cationic iridium(iii) complexes with a triazole–pyridine type ancillary ligand: synthesis, photophysics, electrochemistry properties and piezochromic behavior. J Mater Chem 22(25): 12736-12744.

68. Liao C, Chen H, Su H, Wong K (2011) Tailoring balance of carrier mobilities in solid-state light-emitting electrochemical cells by doping a carrier trapper to enhance device efficiencies. J Mater Chem 21: 17855-17862.

69. Su H, Chen H, Shen Y, Liao C, Wong K, et al. (2011) Highly efficient double-doped solid-state white light-emitting electrochemical cells. J Mater Chem 21(26): 9653-9660.



**DOI:** 10.32474/AOICS.2021.05.000219